Analytical Modeling of Slip Flow in Parallel-plate Microchannels

Navid Kashaninejad^{1*}, Weng Kong Chan¹ and Nam-Trung Nguyen²

¹School of Mechanical and Aerospace Engineering, Nanyang Technological, University, Singapore, 638075, Singapore; ²Queensland Micro and Nanotechnology Centre, Griffith University, Brisbane, 4111, Australia

Abstract: This paper presents analytical modeling of slip liquid flow in parallel-plate microchannels, and can be divided in two parts. In the first part, classical relationships describing velocity, flow rate, pressure gradient, and shear stress are extended to the more general cases where there exist two different values of the yet-unknown slip lengths at the top and bottom walls of the channel. These formulations can be used to experimentally determine the values of slip length on the channels fabricated from two different hydrophobic walls. In the second part, the emphasis is given on the quantification of the slip length analytically. Generating mechanism of slip is attributed to the existence of a low-viscosity region between the liquid and the solid surface. By extending the previous works, the analytical values of slip length are determined using exact, rather than empirical, values of air gap thickness at different ranges of air flow Knudsen number. In addition to the exact expressions of air gap thickness, the corresponding ranges of the channel height where slip flow can be induced are also found analytically. It is found that when the channel height is larger than 700 μm , air flow is in continuum regime and no-slip boundary condition can be used. For the case where the channels height is smaller than 700 μm , and larger than 7.5 μm , slip boundary condition should be used to model the air flow in the channel. Finally, for the channel with the height smaller than 7.5 μm , Navier-Stokes equation cannot be used to model the air flow, and instead molecular-based approaches should be implemented. The results of this paper can be used as a guideline for both experimentalists and theoreticians to study the slip flow in parallel-plate microchannels.

Keywords: ????????????.

1. INTRODUCTION

One of the challenging issues in the domain of micro/nanofluidics is the proper formulation of liquid-solid interaction. Interpretations of the experimental results critically depend on the precise evaluation of the liquid close to the solid wall. Furthermore, deriving the final form of fluid flow in any channels is not possible unless the interactions at the liquid-solid interface, known as boundary conditions (BCs), are well defined. Also, wetting property of a surface represented by a contact angle is an important factor affecting the near-wall liquid flows. Experiments showed that the amount of slip on hydrophobic (low energy) surfaces is much higher than that on hydrophilic ones [1, 2], which were reviewed by Neto et al. [3]. Therefore, it suggests that there should be a relationship between the slip length (microscopic property) and wetting conditions (macroscopic property) of a surface [4]. Slip flow near the channel wall of hydrophobic microchannels can reduce the flow frictional resistance both in laminar [5-8] and turbulent [9-12] regimes. Both smooth [13] and micro/nanopatterned hydrophobic surfaces [14, 15], known as superhydrophobic surfaces, can be fabricated to induce the slip flow.

Lubricating gas layer is considered as one of the possible mechanisms to generate the slip near the hydrophobic surfaces [16]. Accordingly, the existence of this lubricating gas layer, or low-viscosity cushion, can be explained by two different points of view. The first case, termed as recirculating air region, traces back to the early experiment of Ruckstein and Rajora [17] who concluded that there may be a gas gap at the interface between the solid and the liquid caused by the different nature of the two materials. However, the model of gas gap is very strong idealization. In such case, one may expect a totally shear-free BC. In this case, the net flow rate of the gas layer below the liquid flow can be considered to be zero. The second case which is termed reduced viscosity model was first suggested by Vinogradova [18]. According to this model, liquid molecules near hydrophobic surfaces tend to stay in bulk rather than being attracted to the solid wall. Hence, the density of the fluid flow near the hydrophobic surfaces may be reduced compared to the bulk. The theoretical calculations related to this model were performed by Tretheway and Meinhart [19]. To quantify the amount of slip on hydrophobic surfaces Navier slip length is commonly used. It is an unknown parameter needed to be determined experimentally/analytically on both smooth and micropatterned hydrophobic surfaces. There are several direct and indirect methods to measure the amount of this slip length experimentally [20]. One versatile method is to measure the experimental flow rate or average flow velocity in hydrophobic channels and compare it with the theoretical flow rate or average velocity with no-slip BCs. In this case, the final form of theoretical equations describing the flow rate or average velocity with slip BCs is crucial to accurately quantify the slip length. In this paper, first Newtonian liquid flow in parallel-plate microchannels made from two different

channel walls with unequal wettability and surface conditions will be evaluated. The classical formulas for velocity, flow rate, and shear stress will be revised to incorporate the effect of slip velocity near the solid walls in terms of the two different values of slip length on top and bottom walls of the channel. It will be shown that for the limiting case of no-slip BCs at both channel walls, the obtained equations can be simplified to the classical Hagen-Poiseuille theory. These results are more suitable to derive the exact experimental values of slip length on microchannels fabricated from two different channel walls.

Because of the experimental difficulties in determination of slip length, the analytical models devised to quantify this parameter are of great importance. In the second part of this paper, the slip length will be derived theoretically by extending the previous model of reduced viscosity layer near the channel wall by introducing novel expressions to estimate the air gap thickness at different ranges of Knudsen number of gas flow. In addition, the effect of slip flow is considered to be a function of the channel wall, as slip length is always normalized with respect to the channel wall [21]. That explains why slip flow cannot be induced in macro-scale channels to reduce the frictional drag. However, to the best knowledge of the authors, no previous works so far reported the ranges of the channel height where the slip flow is applicable. In this paper, not only the estimated values of the airgap thickness are determined, but the corresponding ranges of the channel height where slip flow is applicable will also be estimated.

2. GENERAL SLIP FLOW IN PARALLEL-PLATE MICROCHANNELS

In previous works, it is always assumed that dominating BCs in liquid flows through microchannels are either no-slip or equal slip conditions. In this section, the general forms of Newtonian liquid flow in parallel-plate microchannel which consists of two different walls with unequal wettabilities and surface conditions are considered. This situation may occur frequently in microchannel fabrication, since fabricating microchannels with a single material is not always possible. In this paper, it is assumed that the width of the channel is much larger than its height so that effect of side walls can be neglected. That means, a high aspect ratio microchannel is investigated. Schematic view of such microchannel is illustrated in (Fig. 1).

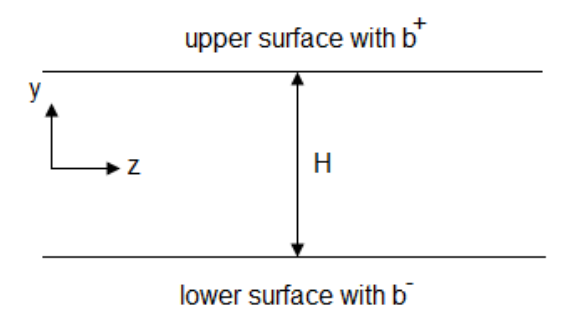


Fig. (1). Schematic view of the channel with different slip lengths at both top and bottom walls.

Considering fully developed laminar flow for Newtonian liquids with constant properties at low Reynolds number, the Navier-Stokes (N-S) equation can be simplified to Stokes equation. Solving this ordinary differential equation, the velocity distribution in terms of BCs can be calculated as follows:

$$\frac{d^2u}{dv^2} = \frac{1}{\mu} \frac{dP}{dz} \Longrightarrow u(y) = \frac{1}{2\mu} \frac{dP}{dz} y^2 + C_1 y + C_2 \tag{1}$$

The corresponding Navier slip BCs at both walls are:

$$\begin{cases} u(y=+h) = -b^{+} \frac{du}{dy} \Big|_{y=+h} \\ u(y=-h) = b^{-} \frac{du}{dy} \Big|_{y=-h} \end{cases}$$
 (2)

Imposing these BCs dictates:

$$\begin{cases} 1/2\mu \frac{dP}{dz}h^2 + C_1h + C_2 = -b^+ \left(1/\mu \frac{dP}{dz}h + C_1\right) \\ 1/2\mu \frac{dP}{dz}h^2 - C_1h + C_2 = b^- \left(-1/\mu \frac{dP}{dz}h + C_1\right) \end{cases} \tag{3}$$

Further simplification of the first BC leads to:

$$C_2 = -\frac{1}{2\mu} \frac{dP}{dz} h(b^+ + b^- + h) + \frac{1}{2} (b^- - b^+) C_1$$
 (4)

Also, the second BC indicates that:

$$\therefore C_1 = \frac{1}{\mu} \frac{dP}{dz} h \frac{(b^- - b^+)}{(2h + b^+ + b^-)}$$
 (5)

Substituting C_1 into the expression of C_2 results in:

$$\therefore C_2 = \frac{1}{2\mu} \left(-\frac{dP}{dz} \right) h \left[\frac{3hb^+ + 3hb^- + 2h^2 + 4b^+b^-}{2h + b^+ + b^-} \right]$$
 (6)

Replacing these constants in Eq. (1) leads to:

$$u(y) = \frac{1}{2\mu} \frac{dP}{dz} y^2 + \frac{1}{\mu} \frac{dP}{dz} h \frac{(b^- - b^+)}{(2h + b^+ + b^-)} y + \frac{1}{2\mu} \left(-\frac{dP}{dz} \right) h \left[\frac{3hb^+ + 3hb^- + 2h^2 + 4b^+ b^-}{2h + b^+ + b^-} \right]$$
(7)

Upon additional simplifications and substituting H = 2h, we can rewrite the obtained Eq. (7) as:

$$u(y) = \frac{1}{\mu} \left(-\frac{d^{p}}{dz} \right) H^{2} \left[-\frac{y^{2}}{2H^{2}} - \frac{(b^{-}-b^{+})}{(H+b^{+}+b^{-})} \frac{y}{2H} + \frac{1}{8H} \frac{3Hb^{+}+3Hb^{-}+H^{2}+8b^{+}b^{-}}{H+b^{+}+b^{-}} \right]$$
(8)

2.1. Dimensionless Form of Velocity Profile

By denoting:

$$u^* = \frac{u}{\frac{1}{\mu} \left(-\frac{dP}{dz}\right)H^2} \tag{9}$$

$$\frac{y}{H} = y^* \tag{10}$$

$$\frac{b}{u} = \beta \tag{11}$$

Eq. (8) can be written in dimensionless form as:

$$u^*(y^*) = -\frac{1}{2}y^{*2} - \frac{(\beta^- - \beta^+)}{(1 + \beta^+ + \beta^-)}y^* + \frac{1}{8} \left[\frac{3\beta^+ + 3\beta^- + 8\beta^+ \beta^- + 1}{\beta^+ + \beta^- + 1} \right]$$
 (12)

2.2. Average Velocity in General Form

In the case of two-wall slip, it is also desirable to calculate the average flow velocity. In particular, the average velocity can be measured experimentally. The average velocity becomes:

$$\overline{u} = \frac{1}{2h} \int_{-h}^{h} u(y) dy = \frac{1}{2h} \int_{-h}^{h} 1/\mu \left(-\frac{dP}{dz} \right) h^{2} \left[-\frac{y^{2}}{2h^{2}} - \frac{(b^{-}-b^{+})}{(2h+b^{+}+b^{-})} \frac{y}{h} + \frac{1}{2h} \frac{3hb^{+} + 3hb^{-} + 2h^{2} + 4b^{+}b^{-}}{2h+b^{+}+b^{-}} \right] dy$$
(13)

After some mathematical manipulations, the average velocity can be expressed as:

$$\bar{u} = \frac{1}{2h} \left[\frac{1}{\mu} \left(-\frac{dP}{dz} \right) h^2 \left[\frac{4h^3 + 8h^2b^- + 8h^2b^+ + 12hb^+b^-}{3h(2h + b^+ + b^-)} \right]$$
 (14)

The final form of the average velocity in terms of the total channel height is formulated in Eq. (15):

$$\dot{u} = \frac{1}{\mu} \left(-\frac{dP}{dz} \right) \left[\frac{H^3 + 4H^2b^- + 4H^2b^+ + 12Hb^+b^-}{12(H+b^++b^-)} \right]$$
 (15)

For the limited case where the intrinsic slip on the upper wall is negligible, $b^+ = 0$, the above equation simplifies to:

$$\bar{u}_{slip} = \frac{1}{\mu} \left(-\frac{dP}{dz} \right) \left[\frac{H^3 + 4H^2b^-}{12(H+b^-)} \right]$$
 (16)

Denoting $\beta^- = b^-/H$, for the case of existing slip on the bottom wall, slip velocity becomes:

$$\bar{u}_{slip} = \frac{1}{12\mu} \left(-\frac{dP}{dz} \right) H^2 \left(\frac{1+4\beta^-}{1+\beta^-} \right)$$
 (17)

where the first term is the no-slip velocity profile traditionally obtained by Hagen-Poiseuille.

2.3. Dimensionless Average Velocity

It is more relevant to normalize the average velocity by $1/\mu (-dP/dz)H^2$ as follows:

$$\therefore \overline{u}^* = \frac{\overline{u}}{\frac{1}{\mu} \left(-\frac{dP}{dz} \right) H^2} = \frac{\frac{1+4\beta^- + 4\beta^+ + 12\beta^+ \beta^-}{12(1+\beta^+ + \beta^-)}}{12(1+\beta^+ + \beta^-)}$$
(18)

2.4. Determination of Slip Flow Rate

Similar to the average velocity, the volumetric flow rate can also be computed as:

$$\dot{u} = \frac{Q}{W} = \frac{1}{\mu} \left(-\frac{dP}{dz} \right) H \left[\frac{H^3 + 4H^2b^- + 4H^2b^+ + 12Hb^+b^-}{12(H+b^++b^-)} \right]$$
 (19)

Alternatively, the dimensionless flow rate in the microchannel can be written as:

$$Q^* = \frac{Q}{\frac{1}{\mu} \left(-\frac{dP}{dz} \right) H^3 W} = \frac{1 + 4\beta^- + 4\beta^+ + 12\beta^+ \beta^-}{12(1 + \beta^+ + \beta^-)}$$
(20)

which is the same as non-dimensional average velocity.

2.5. Determination of Shear Stress and Friction Factor with Slip at the Wall

The shear stress can be calculated as [22]:

$$\tau = \mu \left[\frac{\partial u}{\partial y} + \frac{\partial v}{\partial x} \right] = \mu \frac{\partial u}{\partial y} \tag{21}$$

By substituting the velocity distribution, Eq. (8), shear stress becomes:

$$\dot{\tau} = \mu \frac{\partial u}{\partial y} = (\frac{dP}{dz})H^2 \left[\frac{y}{H^2} + \frac{(b^- - b^+)}{(H + b^+ + b^-)} \frac{1}{2H} \right]$$
 (22)

It is common to define an average wall shear stress as follows:

$$\bar{\tau}_w = \frac{1}{\Gamma} \int_0^{\Gamma} \tau_w \, ds \tag{23}$$

where Γ is the perimeter of the channel and ds is the element of the arc length.

It is possible to relate the average wall shear stress to the required pressure gradient in the channel. Force balance indicates that:

$$dz \int_0^{\Gamma} \tau_w \, ds = -A \, dP \tag{24}$$

Upon replacing the average wall shear stress, i.e. $\int_0^\Gamma \tau_w \, ds = \bar{\tau}_w \Gamma$, the above equation simplifies to:

$$\bar{\tau}_w = \left(-\frac{dP}{dz}\right) \cdot \frac{A}{\Gamma} \tag{25}$$

By comparing the above equation with that of a circular cross section, where $\bar{\tau}_w = (-dP/dz).D/4$, the equivalent diameter for non-circular channel could be defined as:

$$D_h = \frac{4A}{\Gamma} \tag{26}$$

In a parallel-plate microchannel, it is possible to write the hydraulic diameter in terms of channel height and aspect ratio, $\alpha = W/H$,:

$$D_h = \frac{4(H.W)}{2(H+W)} = \frac{2H(W)}{H(1+W/H)} = \frac{2\alpha H}{\alpha + 1}$$
 (27)

Finally the relationship between the wall shear stress and pressure gradient becomes:

$$\bar{\tau}_W = \left(-\frac{dP}{dz}\right) \cdot \frac{D_h}{A} \tag{28}$$

In the present microchannel, the relationship between the pressure gradient and theaverage velocity was obtained. Thus, we can find the relationship between the average wall shear stress and average velocity:

$$\therefore \bar{\tau}_{w} = \frac{6H(H+b^{+}+b^{-})}{H^{3}+4H^{2}b^{-}+4H^{2}b^{+}+12Hb^{+}b^{-}} \cdot \frac{\alpha\mu}{\alpha+1} \cdot U$$
 (19)

Dimensionless shear stress is traditionally called the friction coefficient, C_f , in which shear stress is non-dimensioned by dynamic pressure, $1/2 \rho \bar{u}^2$, as:

$$C_f = \frac{\bar{\tau}_W}{1/2\sigma\bar{u}^2} \tag{30}$$

Also, it is customary to define another dimenstion less friction factor as:

$$f = \frac{8\bar{\tau}_w}{o\bar{u}^2} \tag{31}$$

where f is called Darcy friction factor. It is evident that f is four times in magnitude larger than friction factor C_f .

By substituting the obtained relationship between the average wall shear stress and the pressure gradient, Darcy friction factor becomes:

$$f = \frac{8 \left(-\frac{dP}{dz}\right) D_h/4}{\rho \bar{u}^2}$$
 (32)

which can be written as:

$$f = \frac{(-dP/dz).D_h}{1/2\rho\bar{u}^2}$$
 (33)

In most references, e.g. [23], Darcy friction factor appears once in the following equation:

$$\Delta P = f \, \frac{L}{D_h} \frac{\rho \overline{u}^2}{2} \tag{34}$$

Replacing $(-dP/dz) = \Delta P/L$ in Eq. (33), here the aforementioned equation can be thoroughly proved.

Also, if we define Reynolds number based on the hydraulic diameter, i.e. $Re = \rho \overline{u} D_h / \mu$, Eq. (33) becomes:

$$\therefore f = \frac{\left(-\frac{dP}{dz}\right)D_h^2}{\frac{1}{2}\mu\overline{u}} \times \frac{1}{Re}$$
 (35)

Additionally, from Eq. (15), the relationship between the pressure drop and the average velocity in the microchannel consists of different slip conditions at the top and the bottom walls can be explicitly obtained, as:

$$\left(-\frac{dP}{dz}\right) = \mu \overline{u} \frac{12 \left(H + b^{+} + b^{-}\right)}{H^{3} + 4H^{2}b^{-} + 4H^{2}b^{+} + 12H b^{+}b^{-}}$$
(36)

By substituting this equation into Eq. (35), the friction coefficient becomes:

$$\therefore f = \frac{\frac{24(H+b^{+}+b^{-})}{H^{3}+4H^{2}b^{-}+4H^{2}b^{+}+12Hb^{+}b^{-}} D_{h}^{2}}{Re}$$
(37)

In Eq. (37) by replacing the hydraulic diameter in terms of channel height and aspect ratio, i.e., $D_h = 2\alpha H/(\alpha+1)$, this equation becomes:

$$f = \frac{\frac{24(H+b^{+}+b^{-})}{H^{3}+4H^{2}b^{-}+4H^{2}b^{+}+12Hb^{+}b^{-}} \frac{4\alpha^{2}H^{2}}{(\alpha+1)^{2}}}{Re}$$
(38)

In term of dimensionless slip, i.e., $\beta = b/H$, one can get:

$$\therefore f = \frac{96}{Re} \frac{\alpha^2 (1 + \beta^+ + \beta^-)}{(1 + 4\beta^- + 4\beta^+ + 12\beta^+ \beta^-)(\alpha + 1)^2}$$
(39)

Equivalently, we can also define another dimensionless number by multiplying Darcy friction factor to Reynolds number which is usually called the Poiseuille number:

$$Po = f.Re = 96 \frac{(1+\beta^{+}+\beta^{-})}{(1+4\beta^{-}+4\beta^{+}+12\beta^{+}\beta^{-})(\alpha+1)^{2}}$$
 (40)

The width of the channel is much larger than its height, that is:

$$W \gg H \Rightarrow \frac{W}{H} \gg 1 \to \alpha \gg 1$$
 (41)

The friction factor from the above equation can only be calculated when the aspect ratio is much larger than unity. Sometimes it is completely omitted from the friction factor relation in the case of parallel-plate channels. However, it is retained here for completeness sake. In other words, the obtained formulae are valid for liquid flow through parallel-plate microchannels both for large and relatively moderate aspect ratios.

So far, the general expressions describing the velocity, flow rate as well as friction factor in parallel-plate microchannels were derived in terms of the yet-unknown general slip lengths at both top and bottom channel walls. In the following part, we relate this unknown Navier slip length to the known geometrical parameters of the channel by considering the realistic models causing the slip velocity at the micron scale.

3. APPARENT SLIP IN HYDROPHOBIC MICROCHANNEL

As explained before, one possible reason for the violation of no-slip BC could be the existence of a low-viscosity region very close to the channel wall which is called the apparent slip. The fundamental difference between the apparent and the true slips is shown in (Fig. 2).

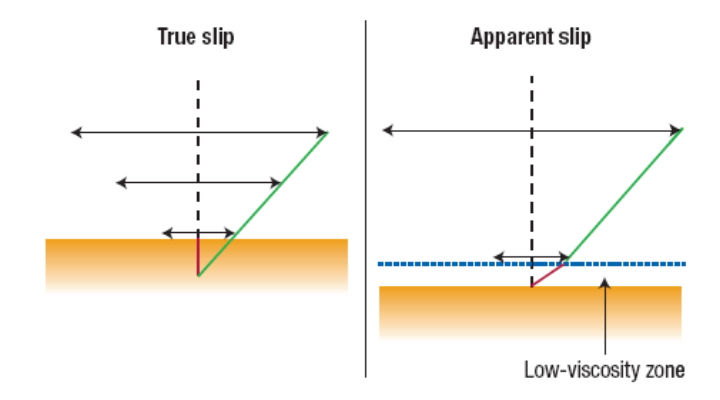


Fig. (2). Two possible mechanisms of slip over low-energy surfaces. Reprinted with permission from [24].

In this section, the apparent slip can be justified due to the existence of a uniform layer of air gap and/or low-viscosity region between bulk liquid flow and solid (non-permeable) surfaces of microchannels whose widths and lengths are much larger than their heights (depths). This model is schematically shown in (Fig. 3).

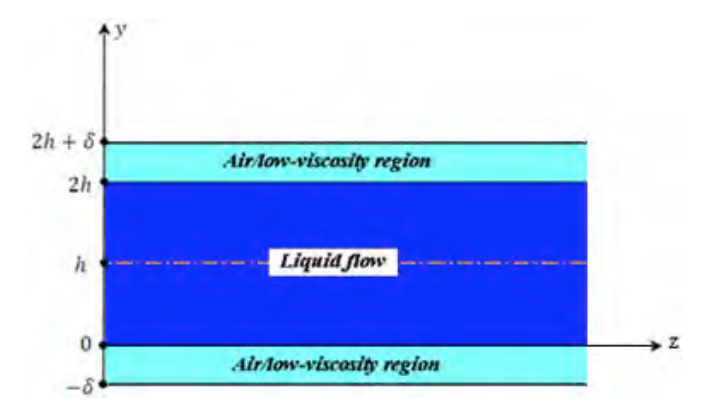


Fig. (3). Two-phase flow in parallel-plate hydrophobic microchannel. Air gap or low viscosity region can explain possible non-sticky behavior of the fluid near the wall.

3.1. Trapped Air Model

In this case, it is assumed that air re-circulates in the vicinity of the wall and the relationship between air region pressure drop and liquid flow can be found from the fact that net flow rate of air flow is zero. The problem is further simplified by assuming: (1) no gravity and no mixing; (2) airliquid interface to be a straight line. In this case, the BC between the gas and the channel wall is assumed to be no-slip. Additionally since both liquid and gas are assumed to be continuum, Eq. (1) can be applied separately for each phase subject to following BCs:

$$BC's: \begin{cases} y = 0: \begin{cases} u_{air} = u_{liquid} \\ \tau_{nt_{air}} = \tau_{nt_{liquid}} \Rightarrow \mu_{liquid} \frac{\partial u_{liquid}}{\partial y} = \mu_{air} \frac{\partial u_{air}}{\partial y} \\ y = -\delta: u_{air} = 0 \\ : \\ y = h: \frac{\partial u_{liquid}}{\partial y} = 0 \end{cases}$$

$$(42)$$

At the interface (y = 0), the velocity and shear stress are assumed to be continuous.

The liquid velocity profile can be calculated as:

$$u_{liquid} = \frac{1}{\mu_{liquid}} \left(-\frac{dP}{dz} \right)_{liquid} h^2 \left(-\frac{1}{2} \left(\frac{y}{h} \right)^2 + \frac{y}{h} + \frac{1}{2} \mu_r \xi \right) \tag{43}$$

where
$$\mu_r = \frac{\mu_{liquid}}{\mu_{air}}$$
 and $\xi = \frac{\delta}{2h}$

Following Navier hypothesis, the effective slip length was calculated as follows:

$$b_{eff} = \frac{1}{4} \mu_r \delta \tag{44}$$

This equation indicates that the effective slip length is related to the viscosity ratio between the liquid and the gas, as well as the height ratio of the air gap and the liquid flow.

3.2 Near Wall Reduced-Viscosity Model

This approach was first adopted by Tretheway and Meinhart [19] who considered the existence of a uniform gas layer near hydrophobic surfaces at both continuum and rarefied gas flow conditions. The main difference between this model and the previous one lies in the pressure drop condition. In this model, known as reduced viscosity model, it is assumed that near wall flows with the same pressure drop as that of the liquid flow. Similar to the velocity profile of the previous case of liquid, the effective slip length can be calculated by the following equations:

$$u_{liquid} = \frac{h^2}{2\mu_{liquid}} \left(-\frac{dP}{dz} \right)_{liquid} \left(-\frac{y^2}{h^2} + \frac{2y}{h} + 4\xi \mu_r + 4\mu_r \xi^2 \right)$$
(45)

$$b_{eff} = \mu_r \delta(1 + \xi) \tag{46}$$

Both Eq. (44) and Eq. (46) depend directly on the thickness of air/low-viscosity δ . Previous results have established the slip lengths without any estimation of the air gap thickness. This limitation will be addressed below by providing some expressions for the air-gap thickness.

3.2.1. Calculation of Air-gap Thickness for Flow at Continuum Region ($Kn \le 10^{-3}$)

Here, we consider a channel with hydrophilic and hydrophobic surfaces at the top and bottom, respectively. It is also assumed that at the interface, due to the small air viscosity, the shear stress is negligible. Hence the BCs become:

$$BC's: \begin{cases} y = -\delta : u_{air} = 0\\ y = 0 : \frac{\partial u_{liquid}}{\partial y} = \frac{\partial u_{air}}{\partial y} = 0\\ y = 2h : u_{liquid} = 0 \end{cases}$$
(47)

By imposing these 4 boundary conditions, the 4 unknowns of air and fluid velocity profiles can be calculated. Air velocity profile becomes:

$$u_{air}(y) = \frac{1}{2\mu_{air}} \left(-\frac{dP}{dz} \right)_{air} \delta^2 \left[1 - \frac{y^2}{\delta^2} \right]$$
 (48)

For the liquid section, similarly we can find:

$$u_{liquid}(y) = \frac{2}{\mu_{liquid}} \left(-\frac{dP}{dz} \right)_{liquid} h^2 \left[1 - \frac{y^2}{4h^2} \right]$$
 (49)

Now, if we assume no velocity jump at the interface, it requires that:

$$u_{liquid}(y=0) = u_{air}(y=0) \tag{50}$$

Substituting Eq. (48) and Eq. (49) into Eq. (50) results:

$$\stackrel{.}{.} \frac{2}{\mu_{liquid}} \left(\frac{dP}{dz}\right)_{liquid} h^2 = -\frac{1}{2\mu_{air}} \delta^2 \left(\frac{dP}{dz}\right)_{air}$$
 (51)

For equal pressure gradient at both phases (reducedviscosity approach), the above equation simplifies to:

$$4/\mu_r h^2 = \delta^2 \tag{52}$$

Hence, the thickness of the reduced viscosity zone must

$$\delta = \sqrt{\frac{4h^2}{\mu_r}} \tag{53}$$

It is noted that the above equation is valid for the Knudsen number less than 0.001.

$$Kn = \frac{\ell}{\delta} \Longrightarrow \delta = \frac{\ell}{Kn}$$
 (54)

At sea level, the mean free path of air, ℓ , is in the order of $0.1~\mu m$. Accordingly, the minimum air gap thickness, δ_{min} ,

$$\delta_{min} = \frac{\ell}{(Kn)_{max}} = \frac{0.1 \,\mu m}{0.001} = 100 \,\mu m \tag{55}$$

Hence, the minimum allowable height of the microchannel in this case should be:

$$H_{min} = \sqrt{\mu_r} \delta_{min} \cong 700 \ \mu m \tag{56}$$

3.2.2 Calculation of Air-gap Thickness for Flow at Slip Region $(10^{-3} \le \text{Kn} \le 10^{-1})$

In this case, slip exists between the air molecules and the solid surface. To quantify the amount of slip of gases, Maxwell first used the general Navier slip model as follows:

@ wall:
$$u_{air} - u_{solid} = \epsilon \xrightarrow{\partial u_{air}} \xrightarrow{stationary\ wall} u_{air} = \epsilon \xrightarrow{\partial u_{air}} (57)$$

We will later discuss the values of slip length for air and solid surface (ϵ) . At the moment, it is assumed to be a known parameter. Then, the BCs become:

$$BC's: \begin{cases} y = -\delta : u_{air} = \epsilon \frac{\partial u_{air}}{\partial y} \\ y = 0 : \frac{\partial u_{liquid}}{\partial y} = \frac{\partial u_{air}}{\partial y} = 0 \\ y = 2h : u_{liquid} = 0 \end{cases}$$
 (58)

By imposing these four BCs, the corresponding velocity profiles for air and liquid can be found:

$$u_{air}(y) = \frac{1}{2\mu_{air}} \left(\frac{dP}{dz}\right)_{air} y^2 + C_5$$
 (59)

$$\therefore C_5 = \frac{-1}{2\mu_{air}} \left(\frac{dP}{dz}\right)_{air} \delta^2 \left[1 + 2\frac{\epsilon}{\delta}\right]$$
Finally, air velocity profile becomes:

$$u_{air}(y) = -1/2\mu_{air} \left(\frac{dP}{dz}\right)_{air} \delta^2 \left[1 + 2\frac{\epsilon}{\delta} - \frac{y^2}{\delta^2}\right]$$
 (61)

For the liquid velocity, the equation remains the same as before:

$$u_{liquid}(y) = -2/\mu_{liquid} \left(\frac{dP}{dz}\right)_{liquid} h^2 \left[1 - \frac{y^2}{4h^2}\right]$$
 (62)

Again, if we assume no velocity jump between air and liquid at the interface, it requires that:

$$^{-1}/_{2\mu_{air}}\left(\frac{dP}{dz}\right)_{air}\delta^{2}\left[1+2\frac{\epsilon}{\delta}\right] = ^{-2}/_{\mu_{liquid}}\left(\frac{dP}{dz}\right)_{liquid}h^{2} \qquad (63)$$

For equal pressure gradient at both phases (reduced-viscosity approach), the two pressure drops should be the same, so Eq. (63) simplifies to:

$$\delta^2 + 2\epsilon \,\delta - \frac{4}{\mu_r} h^2 = 0 \tag{64}$$

Eq. (64) is a quadratic equation for δ , therefore, the airgap height can be computed as:

$$\delta = -\epsilon \pm \sqrt{\epsilon^2 + \frac{4}{\mu_r} h^2} \tag{65}$$

Because the air-gap cannot be negative, the negative sign before the square root is not acceptable:

$$\delta = -\epsilon + \sqrt{\epsilon^2 + \frac{4}{\mu_r} h^2} \tag{66}$$

If we assume no-slip at the wall, as in the previous case, the same formula describing the air-gap height can be obtained, i.e. Eq. (53):

$$\delta_{\epsilon \to 0} = 0 + \sqrt{0 + \frac{4}{\mu_r} h^2} = \sqrt{\frac{4h^2}{\mu_r}} \tag{67}$$

The maximum allowable Knudsen number in this case should not exceed 0.1, it requires that:

$$\delta_{min} = \frac{\ell}{(Kn)_{max}} = \frac{0.1 \,\mu m}{0.1} = 1 \,\mu m \tag{68}$$

From Eq. (66), the height of the channel (2h) can be found in terms of gap-height:

$$2h = \sqrt{\mu_r \left[1 + 2\frac{\epsilon}{\delta} \right]} \delta \tag{69}$$

To find the minimum height of the channel, we need to find the typical value of ϵ . Accordingly, the Maxwell equation can be used:

$$\epsilon = \left(\frac{2-\sigma}{\sigma}\right)\left(\frac{2}{3}\ell\right) \tag{70}$$

where σ is the tangential momentum accommodation coefficient. This parameter is a function of the solid material, gas type and surface roughness. The experiments suggest that σ should range from 0.5 to 1. The maximum value $\sigma=1$ is typical for most surfaces, while the minimum $\sigma=0.5$ is for very smooth surface with roughness height in the order of nanometers.

Therefore, σ can be approximated as unity, so the slip length of air and solid surface becomes:

$$\epsilon_{air} = \left(\frac{2}{3}\ell\right) \xrightarrow{\ell=0.1 \, \mu m} \epsilon_{air} = 0.0667 \, \mu m \tag{71}$$

Finally, the minimum height of the channels can be obtained from Eq. (69):

$$(2h)_{min} = \sqrt{\mu_r \left[1 + 2 \frac{\epsilon}{\delta_{min}} \right]} \, \delta_{min} \, \cong 7 \times \sqrt{1 + \frac{2 \times 0.0667 \, \mu m}{1 \, \mu m}} \times 1 \mu m \approx 7.523 \mu m$$
(72)

Therefore, the range of the channel height for the model to be valid is:

$$7.5 \ \mu m < H < 700 \ \mu m$$
 (73)

which corresponds to an air-gap in the range of:

$$1 \,\mu m < \delta < 100 \,\mu m \tag{74}$$

According to the obtained results, not only the estimated values of the air-gap thickness were determined, but the related range of the channel height was also estimated. It was found that when the channel height is larger than $700 \, \mu m$, air flow is in continuum regime and no-slip BC for air flow can be used. For the case where the channels height is smaller than $700 \, \mu m$ and larger than $7.5 \, \mu m$, slip BC should be used to model the air flow in the channel. Finally, for the channel with the height smaller than $7.5 \, \mu m$, the N-S equation cannot be used to model the air flow and molecular-based approaches should be used. The key findings of this section can be summarized in the Table 1.

As a worked example, we consider the specifications of laser fabricated polymethylmetacrylate (PMMA) microchannels in our previous work [25] with 4.19 mm width and 57 mm length while the channel height varied from 285 μm to 1083 μm . For the case with higher channel height since $H > 700 \mu m$, air flow can be considered in continuum re-

Table 1. Summary of the obtained analytical results of hydrophobic microchannels with reduced viscosity gas region assumption.

	Continuum Region	Slip Region
Effective slip length	$b_{eff} = \mu_r \delta(1+\xi)$	$b_{eff} = \mu_r \delta(1+\xi)$
Air gap thickness	$\delta = \sqrt{\frac{4h^2}{\mu_r}}$	$\delta = -\epsilon + \sqrt{\epsilon^2 + \frac{4h^2}{\mu_r}}$
Range of air gap	$\delta \geq 100~\mu m$	$1 \mu m < \delta < 100 \mu m$
Channel height	<i>H</i> ≥ 700 μm	$7.5 \ \mu m < H < 700 \ \mu m$

gion with $\epsilon = 0$. Accordingly, from Eq. (53) the air gap thickness becomes $\delta = \sqrt{1083^2/49} = 154 \,\mu m$ $\xi = \delta/H = 0.143$. Substituting these values in Eq. (46), the effective slip length in this case becomes: $b_{eff} = 49 \times$ $0.154(1 + 0.143) = 8.625 \, mm$. This shows that when the channel height is larger than 1 mm, to induce the slip liquid flow the lower channel wall should be in such a hydrophobic state to generate the air gap thickness more than 150 μm . In practice, engineered superhydrophobic surfaces rather than smooth hydrophobic surfaces may generate this air gap thickness. For the second channel where the height is less than 700 μm , the air flow should be modeled in slip region with $\epsilon = 0.0667 \, \mu m$. Then, from Eq. (66) the air gap thickness becomes: $\delta = -0.0667 + \sqrt{0.0667^2 + 285^2/49} = 40 \,\mu m$, and $\xi = \delta/H = 0.143$. Finally the effective slip length should be: $b_{eff} = 49 \times 0.154(1 + 0.143) = 2.24 \text{ mm}$. As these examples illustrate, using the reduced viscosity model predicts the effective slip length in the order of millimeter while in practice slip length in the order of hundreds of nanometers is reported. Although in this paper, the expressions to predict the effective slip length along with air gap thickness are provided, it shows that the reduced viscosity model is a strong idealization model of slip and predicts the maximum possible drag reduction efficiency of hydrophobic microchannels.

4. CONCLUSIONS

Analytical modeling of liquid flow in parallel-plate microchannels was presented. First, classical relationships describing velocity, flow rate, pressure gradient, and shear stress were extended to the more general cases where there existed two different values of yet-unknown slip length at the top and bottom walls of the channel. Subsequently, the analytical estimation of the slip length was proposed. Previous works where the generating mechanism of slip was attributed to the existence of a low-viscosity region between the liquid and the solid surfaces were further extended. In particular, two different cases were considered based on the pressure gradient: a) re-circulating air region, where the net flow rate of gas phase was zero; b) reduced viscosity gas region, in which pressure gradient was assumed to be the same at both phases. It was found that the slip length in both cases was directly proportional to the ratio of liquid-to-gas viscosity as well as the air gap thickness. Therefore, it was necessary to estimate the air gap thickness to quantify the value of slip length. Unlike other studies which used empirical values of air gap thickness, here, equations describing this parameter were derived based on different ranges of Knudsen number for the case of reduced viscosity region. Following this approach, the ranges of microchannel height where slip flow becomes more pronounced were analytically estimated, Table 1. These results can be used to find the values of slip length both experimentally, the first part, and analytically, the second part of this paper.

CONFLICT OF INTEREST

The authors confirm that this article content has no conflicts of interest.

ACKNOWLEDGEMENTS

Declared none.

REFERENCES

- Tretheway D.C. and C.D. Meinhart, Apparent fluid slip at hydrophobic microchannel walls. Physics of Fluids, 14 (2002), pp.
- [2] Choi C.H., K.J.A. Westin, and K.S. Breuer, Apparent slip flows in hydrophilic and hydrophobic microchannels. Physics of Fluids, 15 (2003), pp. 2897.
- Neto C., D.R. Evans, E. Bonaccurso, H.J. Butt, and V.S.J. Craig, Boundary slip in Newtonian liquids: a review of experimental studies. Reports on Progress in Physics, 68 (2005), pp. 2859.
- [4] Voronov R.S., D.V. Papavassiliou, and L.L. Lee, Review of fluid slip over superhydrophobic surfaces and its dependence on the contact angle. Industrial & Engineering Chemistry Research, 47 (2008), pp. 2455-2477.
- Ou J., B. Perot, and J.P. Rothstein, Laminar drag reduction in microchannels using ultrahydrophobic surfaces. Physics of Fluids, 16 (2004), pp. 4635.
- [6] Hao P.F., C. Wong, Z.H. Yao, and K.Q. Zhu, Laminar Drag Reduction in Hydrophobic Microchannels. Chemical Engineering & Technology, 32 (2009), pp. 912-918.
- Kashaninejad N., N.-T. Nguyen, and W.K. Chan, Eccentricity [7] effects of microhole arrays on drag reduction efficiency of microchannels with a hydrophobic wall. Physics of Fluids, 24 (2012), pp. 112004-18.
- UDAGAWA H., Drag reduction of Newtonian fluid in a circular pipe with a highly water-repellent wall. J. Fluid Mech, 381 (1999), pp. 225-238.
- [9] Daniello R.J., N.E. Waterhouse, and J.P. Rothstein, Drag reduction in turbulent flows over superhydrophobic surfaces. Physics of Fluids, 21 (2009), pp. 085103.
- [10] Martell M.B., J.P. Rothstein, and J.B. Perot, An analysis of superhydrophobic turbulent drag reduction mechanisms using direct numerical simulation. Physics of Fluids, 22 (2010), pp. 065102.
- [11] Fukagata K., N. Kasagi, and P. Koumoutsakos, A theoretical prediction of friction drag reduction in turbulent flow by superhydrophobic surfaces. Physics of Fluids, 18 (2006), pp.
- [12] Gogte S., P. Vorobieff, R. Truesdell, A. Mammoli, F. van Swol, P. Shah, and C.J. Brinker, Effective slip on textured superhydrophobic surfaces. Physics of Fluids, 17 (2005), pp. 051701-4.
- Cottin-Bizonne C., B. Cross, A. Steinberger, and E. Charlaix, Boundary slip on smooth hydrophobic surfaces: Intrinsic effects and possible artifacts. Physical review letters, 94 (2005), pp.
- [14] Kashaninejad N., W.K. Chan, and N.-T. Nguyen, Eccentricity Effect of Micropatterned Surface on Contact Angle. Langmuir, 28 (2012), pp. 4793-4799.
- Kashaninejad N., N.-T. Nguyen, and W.K. Chan, The three-phase contact line shape and eccentricity effect of anisotropic wetting on hydrophobic surfaces. Soft Matter, 9 (2013), pp. 527-535.
- [16] Lauga E. and M.P. Brenner, Dynamic mechanisms for apparent slip on hydrophobic surfaces. Physical Review E, 70 (2004), pp.
- [17] Ruckenstein E. and P. Rajora, On the no-slip boundary condition of hydrodynamics. Journal of colloid and interface science, 96 (1983),
- [18] Vinogradova O.I., Drainage of a thin liquid film confined between hydrophobic surfaces. Langmuir, 11 (1995), pp. 2213-2220.
- [19] Tretheway D.C. and C.D. Meinhart, A generating mechanism for apparent fluid slip in hydrophobic microchannels. Physics of Fluids, 16 (2004), pp. 1509-1515.
- [20] Lauga E., M.P. Brenner, and H.A. Stone, Microfluidics: the no-slip boundary condition. Handbook of Experimental Fluid Dynamics (Chapter 19), J Foss, C Tropea, AL Yarin (Eds.), Springer (2007), pp. 1219-1240.
- [21] Rothstein J.P., Slip on superhydrophobic surfaces. Annual Review of Fluid Mechanics, 42 (2010), pp. 89-109.
- [22] White F.M., Viscous fluid flow. 2 (1991).

- [23] Sharp K.V., Experimental investigation of liquid and particle-laden flows in microtubes, 2001, University of Illinois at Urbana-Champaign: United States -- Illinois. pp. 247.
- [24] Granick S., Y. Zhu, and H. Lee, *Slippery questions about complex fluids flowing past solids*. Nature Materials, 2 (2003), pp. 221-227.

[25] Kashaninejad N., W.K. Chan, and N.-T. Nguyen, Fluid mechanics of flow through rectangular hydrophobic microchannels. ASME conference proceedings 2011 (44632), pp. 647-655.

Received: February 01, 2013 Revised: April 12, 2013 Accepted: May 27, 2013